LA-UR-21-24977

Title:	Theoretical justification for heat flux limiter 0.15
Author(s):	Sadler, James David
Intended for:	Report
Issued:	2021-05-24

Theoretical justification for heat flux limiter 0.15

James Sadler

May 10, 2021

In this section, we describe a semi-nonlocal kinetic model for the electron heat flux. The model has no free parameters. It takes the more physically motivated approach of placing a limiter on the perturbation to the electron distribution function, rather than the usual ad-hoc limiter on the heat flux. If the kinetic model is fitted by a heat flux limiter model, we find that the higher value of $f_e = 0.15$ is a much closer fit than other models with $f_e \simeq 0.02$.

In the local transport model, assuming a weakly coupled plasma with Coulomb logarithm $\ln \Lambda \gg 1$, the electron heat flux is given by the Spitzer-Härm heat flux [1]. This breaks down when the temperature gradient becomes so steep that the electron transport is non-local, meaning that the Knudsen nonlocality parameter $K_N = \lambda_{\mathrm{mfp}} |\nabla T_e| / T_e$ approaches one. This expression contains the electron temperature T_e and electron Coulomb mean free path

$$\lambda_{\mathrm{mfp}} = 2.5 \times 10^{-13} \frac{A}{Z^2 \ln \Lambda} \left(\frac{T_e}{\mathrm{eV}} \right)^2 \left(\frac{\rho}{\mathrm{gcm}^{-3}} \right)^{-1} \mathrm{m}, \tag{1}$$

where ρ is the mass density, A is the ion atomic mass number and Z is the ion charge state. K_N is the ratio of the mean free path to the temperature gradient scale-length.

The heat flux can be found from the electron Vlasov-Fokker-Planck equation

$$\frac{\partial f_e}{\partial t} + \mathbf{v} \cdot \nabla f_e - \frac{e}{m_e} \mathbf{E} \cdot \frac{\partial f_e}{\partial \mathbf{v}} = \mathbf{C}_{ee} + \mathbf{C}_{ei}, \tag{2}$$

where $f_e(t, \mathbf{x}, \mathbf{v})$, $\mathbf{v}$, $-e$, m_e, n_e are the electron distribution function, velocity, charge, mass and number density, respectively. $\mathbf{E}$ is the electric field, $\mathbf{C}_{ee}$ is the electron-electron collision operator and $\mathbf{C}_{ei}$ is the electron-ion collision operator. Magnetic fields have been neglected. Spatial gradients and electric fields drive the distribution away from Maxwellian, whereas collisions restore it to Maxwellian.

It is helpful to make the local approximation that collisions are strong, meaning f_e can be set as approximately isotropic Maxwellian $f_M(v, T_e, n_e) = n_e(\sqrt{\pi} v_{th})^{-3} \exp(-y^2)$, where $v = |\mathbf{v}|$, $y = v/v_{th}$ and the electron thermal speed $v_{th} = \sqrt{2T_e/m_e}$. We introduce a small perturbation $\mathbf{f}_1(v)$, such that $f_e = f_M + \mathbf{f}_1 \cdot \mathbf{v}/v$. This perturbation is a vector quantity and it has a spatial direction, such that the distribution can now have an overall flow. This will

allow us to find the flow of charge and heat induced by a temperature gradient or electric field. In the ion fluid rest frame, the perturbation reaches a steady state given by [2, 3, 4]

$$y \nabla f_M - \frac{e}{m_e v_{th}} \mathbf{E} \frac{\partial f_M}{\partial v} = -\frac{\mathbf{f}_1}{\lambda_{\mathrm{mfp}} y^3}. \tag{3}$$

In this equation, we have neglected the electron-electron collision operator and retained only the electron-ion collisions on the right hand side. Due to the Z^2 dependence of electron-ion collisions, this is valid only in the limit $Z \to \infty$. The electron-electron collision operator for $\mathbf{f}_1$ is much more complex [2]. Furthermore, it is usually smaller in magnitude than the electron-ion collisions, so it will not change the results by much. We therefore expect the heat flux result to be valid for $Z \to \infty$, and electron-electron collisions will change it by a factor of $\simeq 2$ for $Z \simeq 1$. The derivatives of a Maxwellian distribution are

$$\nabla f_M = \frac{f_M}{n_e} \nabla n_e + \left(y^2 - \frac{3}{2} \right) \frac{f_M}{T_e} \nabla T_e, \quad \frac{\partial f_M}{\partial v} = -\frac{2y}{v_{th}} f_M. \tag{4}$$

This leads to the perturbation

$$\mathbf{f}_1 = -y^4 f_M \lambda_{\mathrm{mfp}} \left(\frac{e\mathbf{E}}{T_e} + \frac{\nabla n_e}{n_e} + \left(y^2 - \frac{3}{2} \right) \frac{\nabla T_e}{T_e} \right) \tag{5}$$

The electron current can be found from the velocity moment of the distribution function

$$\mathbf{J} = -\frac{4\pi e}{3} \int_0^\infty \mathbf{f}_1 v^3 \, dv = 0. \tag{6}$$

This expression can be derived [2] by substituting $f_e = f_M + \mathbf{v} \cdot \mathbf{f}_1 / v$ into the definition of the electron current $\mathbf{J} = -e \int f_e \mathbf{v} d^3 \mathbf{v}$. There is one factor of v from the definition of current, and also a factor of v^2 from the spherical coordinates Jacobian. Assuming there are no magnetic fields, the steady state Amperes law means that $\mathbf{J} = 0$. Oscillations on the electron timescale damp away, and the electric field $\mathbf{E}$ reaches an equilibrium ambipolar value such that $\mathbf{J} = 0$ and Eq. (6) is satisfied. Substituting Eq. (5) into Eq. (6) and completing the Gaussian integrals gives this value as

$$\mathbf{E} = -\frac{T_e \nabla n_e}{n_e e} - \frac{5}{2} \frac{\nabla T_e}{e} = -\frac{\nabla(n_e T_e)}{n_e e} - \frac{3}{2} \frac{\nabla T_e}{e}. \tag{7}$$

This contains the electron pressure term and the thermoelectric temperature gradient term. Substituting Eq. (7) into Eq. (5), the ambipolar Spitzer perturbation is then simply

$$\mathbf{f}_{1,S} = -\left(y^6 - 4y^4 \right) \lambda_{\mathrm{mfp}} \frac{\nabla T_e}{T_e} f_M \tag{8}$$

This is plotted in Fig. 1a with the green line, and compared to the background Maxwellian f_M in blue. The perturbation has a complex shape, with a flow
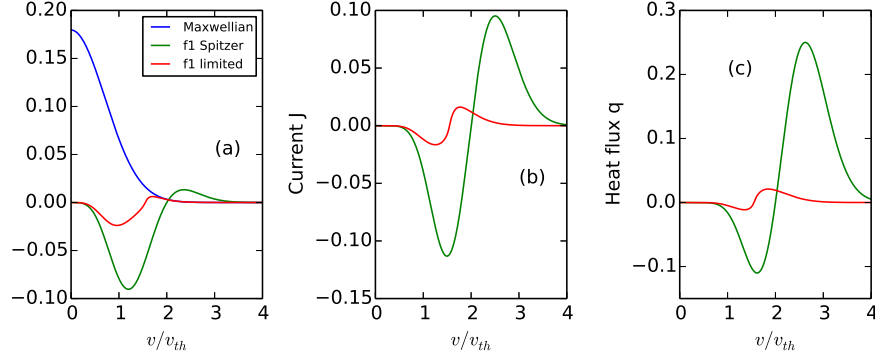
Figure 1: (a) Plots of the isotropic Maxwellian f_M (blue) with the Spitzer anisotropic perturbation (green) in a temperature gradient with nonlocality $K_N = 0.4$. This is unphysical because it exceeds f_M at high velocity, so a limited perturbation with $f_1 < f_M$ (red) should be more accurate. (b) The current caused by the anisotropy in the two models (arbitrary units). (c) The heat flux caused by the anisotropy in the two models (arbitrary units).

of high velocity electrons at $v \simeq 2.5 v_{th}$. However, to keep the overall current zero, there must be a return current of cold electrons at $v \simeq v_{th}$. The resulting current in Eq. (6), $\propto \mathbf{f}_1 v^3$, is shown in Fig. 1b. The electric field takes a value such that the return current of cold electrons precisely matches the flow of hot electrons down the temperature gradient, such that $\int \mathbf{f}_1 v^3 \, dv = 0$. The heat flux, proportional to the higher moment $\mathbf{f}_1 v^5$, is plotted in Fig. 1c. It is weighted more towards the faster electrons. As a result, there is an overall heat flux down the temperature gradient, carried by faster electrons with $v \simeq 2.7 v_{th}$.

Integrating this curve [2] gives the overall heat flux $\mathbf{q}_e = (4\pi m_e/3) \int_0^\infty \mathbf{f}_1 v^5 \, dv$. The result is the Spitzer heat flux $\mathbf{q}_S$, given by

$$|\mathbf{q}_S| = \frac{2m_e}{3} v_{th}^3 \frac{|\nabla T_e|}{T_e} \frac{\lambda_{\mathrm{mfp}} n_e}{\sqrt{\pi}} \int_0^\infty y^9 (y^2 - 4) e^{-y^2} \, dy = \frac{16}{\sqrt{\pi}} K_N q_{\mathrm{fs}}. \qquad (9)$$

This result is plotted with the solid line in Fig. 2. The Spitzer heat flux is written in terms of the free streaming heat flux $q_{\mathrm{fs}} = n_e T_e v_{th}$, which is equivalent to the energy flux if all of the electrons move in the same direction at the average thermal speed $v_{th} = \sqrt{2T_e/m_e}$. The Spitzer flux is also directly proportional to the nonlocality parameter K_N, containing the temperature gradient. For general Z, the Spitzer heat flux is $|\mathbf{q}_S| = (3\sqrt{\pi}/8)\kappa_\parallel(Z) K_N q_{fs}$, where $\kappa_\parallel(Z)$ is the transport coefficient, given in ref. [4].

Clearly the Spitzer theory breaks down if $K_N \simeq 1$, since the heat flux cannot exceed the free streaming limit. This can also be seen in Fig. 1a, since the perturbation is larger than f_M when $K_N \simeq 1$. Physically, we must have $f_e > 0$ and so the perturbation must be less than the Maxwellian $|\mathbf{f}_1| < |f_M|$.
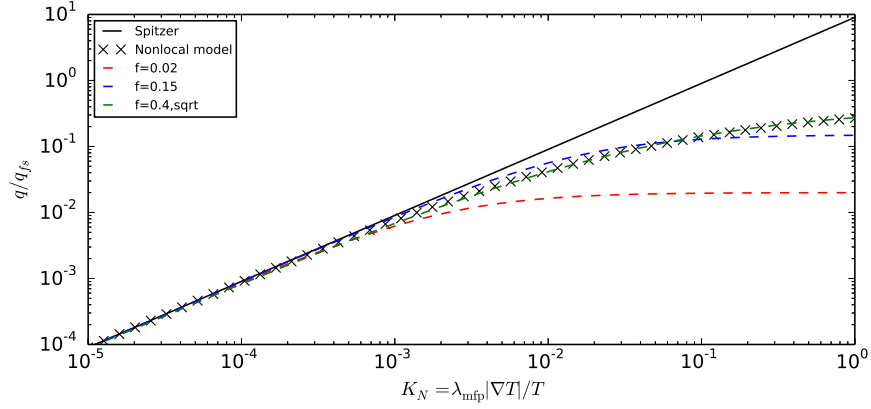
3

Figure 2: Plots of the heat flux (normalized to the free streaming flux $q_{\mathrm{fs}} = n_e T_e \sqrt{2T_e/m_e}$) versus the temperature gradient. The temperature gradient is written in a dimensionless form as the nonlocality parameter $K_N = \lambda_{\mathrm{mfp}}|\nabla T_e|/T_e$. The solid line is the Spitzer model, which breaks down for high K_N. The semi-nonlocal kinetic results (crosses) are fitted by a flux limiter model Eq. (11) with $f_e = 0.02$ or $f_e = 0.15$. The best fit is using Eq. (12) with $f_e = 0.4$. Results are shown for $Z \to \infty$ and are expected to vary by a factor $\simeq 10$ for $Z \simeq 1$.

Considering Eq. (8), there are always some electrons with $y \gg 1$ that lead to $|\mathbf{f}_1| > f_M$. This is due to the inadequacy of the f_M, $\mathbf{f}_1$ expansion, and higher order terms are needed to keep f_e positive everywhere. However, at $y \gg 1$, $\mathbf{f}_1$ is exponentially small and so this breakdown of the theory does not affect the heat flux too much when $K_N \ll 1$. The Spitzer result only becomes significantly wrong when $|\mathbf{f}_1| \simeq f_M$ in the heat flux region with $y \simeq 3$. Setting $|\mathbf{f}_1| = f_M$ in Eq. (8) with $y = 3$, we find an upper limit for the validity of the Spitzer heat conductivity $K_N \simeq (y^6 - 4y^4)^{-1} = 0.0024$. Due to the faster, less collisional electrons carrying the heat flux, the Spitzer theory starts to break down at $K_N \ll 1$.

In reality, at this point, f_e becomes non-Maxwellian and higher order terms are needed in the expansion. This results in the full nonlocal heat flux model, e.g. [5]. However, a simpler and physically motivated fix to the Spitzer model is to retain the f_M, $\mathbf{f}_1$ expansion and simply limit the size of $\mathbf{f}_1$ to be $|\mathbf{f}_1| < f_M$, such that f_e remains positive everywhere. This requires imposing a perturbation limiter so that

$$\tilde{\mathbf{f}}_1 = \frac{\mathbf{f}_1}{1 + |\frac{\mathbf{f}_1}{f_M}|}, \tag{10}$$

where $\mathbf{f}_1$ is given by Eq. (5) and $\tilde{\mathbf{f}}_1$ is the limited perturbation. However, this limiter changes the current $\mathbf{J} \propto \int \tilde{\mathbf{f}}_1 v^3 \, dv$, so then a different $\mathbf{E}$ value is needed

4

to make $\mathbf{J} = 0$ and the Spitzer value Eq. (7) is no longer correct. In general, for a given value of K_N, Eqs. (10), (5) and (6) must be numerically iterated to find the correct $\mathbf{E}$ value that gives $\mathbf{J} = 0$. This gives the equilibrium solution shown in Fig. 1a. For $K_N \ll 1$, $\tilde{\mathbf{f}}_1$ is equal to the Spitzer perturbation $\mathbf{f}_{1,S}$. However, for larger K_N, it is significantly less. Fig. 1 shows the case with $K_N = 0.4$. Notice how the tail of $\tilde{\mathbf{f}}_1$ has been cut down by the limiter, so that it is less than f_M. However, the slower part of $\mathbf{f}_1$ is also affected, since now not as much return current is needed to balance the current of the fast electrons. The current of this $\tilde{\mathbf{f}}_1$ distribution is shown in Fig 1b. The return flux of colder electrons still exactly balances the forward flux of hot electrons. However, the magnitudes of these fluxes are less. The resulting heat flux is shown in Fig 1c. Although there is still a positive heat flux, it is significantly less than that predicted by the Spitzer perturbation. The limiting of $\tilde{\mathbf{f}}_1$ to be less than f_M therefore significantly reduces the heat flux below the Spitzer prediction. However, for $K_N \ll 1$, the limiter is not active and we have $\tilde{\mathbf{f}}_1 \to \mathbf{f}_{1,S}$.

The heat flux of this semi-nonlocal model is shown in Fig. 2 with the crosses. For $K_N \ll 1$, it agrees with the Spitzer model. However, the numerical solution diverges away from q_S at higher nonlocality, and it does not exceed q_{fs}. The deviation first starts to occur at $K_n \simeq 0.002$, as predicted earlier.

Typically in simulation codes, the heat flux is fitted by a limiter of a similar form to Eq. (10), given by

$$\mathbf{q} = \mathbf{q}_S \left(1 + \frac{|\mathbf{q}_S|}{f_e q_{fs}} \right)^{-1}, \tag{11}$$

where the constant f_e is known as the heat flux limiter. This model is shown in red for $f_e = 0.02$ and blue for $f_e = 0.15$. It is clear that the $f_e = 0.15$ model is significantly closer to the kinetic results. A least squares optimization of the relative errors found an optimal value of $f_e = 0.18$. An even better fit is given by

$$\mathbf{q} = \mathbf{q}_S \left(1 + \sqrt{\frac{|\mathbf{q}_S|}{f_e q_{fs}}} \right)^{-2}, \tag{12}$$

with $f_e = 0.4$. This model is shown by the green dashed line in Fig. 2.

References

[1] L. Spitzer Jr and R. Härm, "Transport phenomena in a completely ionized gas," *Physical Review*, vol. 89, no. 5, p. 977, 1953.

[2] A. Thomas, M. Tzoufras, A. Robinson, R. Kingham, C. Ridgers, M. Sherlock, and A. Bell, "A review of vlasov–fokker–planck numerical modeling of inertial confinement fusion plasma," *Journal of Computational Physics*, vol. 231, no. 3, pp. 1051–1079, 2012.

[3] S. Braginskii, "Transport phenomena in a completely ionized two-temperature plasma," *Sov. Phys. JETP*, vol. 6, no. 33, pp. 358–369, 1958.

[4] E. Epperlein and M. Haines, "Plasma transport coefficients in a magnetic field by direct numerical solution of the fokker–planck equation," *The Physics of fluids*, vol. 29, no. 4, pp. 1029–1041, 1986.

[5] G. Schurtz, P. D. Nicolaï, and M. Busquet, "A nonlocal electron conduction model for multidimensional radiation hydrodynamics codes," *Physics of plasmas*, vol. 7, no. 10, pp. 4238–4249, 2000.